

# Double dispersion of the magnetic resonant mode in cuprates from the memory function approach

I. Sega<sup>1</sup> and P. Prelovšek<sup>1,2</sup>

<sup>1</sup>*J. Stefan Institute, SI-1000 Ljubljana, Slovenia*

<sup>2</sup>*Faculty of Mathematics and Physics, University of Ljubljana, SI-1000 Ljubljana, Slovenia*

(Received 16 February 2005; published 31 March 2006)

The magnetic excitation spectra in the vicinity of the resonant peak, as observed by inelastic neutron scattering in cuprates, are studied within the memory-function approach. It is shown that at intermediate doping the superconducting gap induces a double dispersion of the peak, with an anisotropy rotated between the downward and upward branch. Similar behavior, but with a spin-wave dispersion at higher energies, is obtained for the low-doping case assuming a large pairing pseudogap.

DOI: [10.1103/PhysRevB.73.092516](https://doi.org/10.1103/PhysRevB.73.092516)

PACS number(s): 74.72.Bk, 71.27.+a, 74.20.Mn, 74.25.Ha

The magnetic resonant mode, first observed in the superconducting (SC) phase of  $\text{YBa}_2\text{Cu}_3\text{O}_{6+x}$  (YBCO),<sup>1</sup> has been in the last decade the subject of numerous studies, with the essential information coming from the inelastic neutron scattering (INS) experiments.<sup>2,3</sup> It has been found that the peak intensity is highest at the commensurate wave vector  $\mathbf{Q} = (\pi, \pi)$ , while its frequency  $\omega_r$  shifts with doping. More recently, detailed studies of the magnetic response in the vicinity of the resonant peak (RP) revealed several intriguing but quite universal features. While in the SC YBCO the stronger component of the resonant mode disperses downwards,<sup>4</sup> another branch apparently emerging from the same peak shows upward dispersion.<sup>5-7</sup> Similar features have been observed in the underdoped YBCO, wherein the upper branch evolves into a spin-wavelike mode at higher energies.<sup>8,9</sup> It is quite remarkable that dispersions for various doping show quite consistent anisotropic intensity within the  $\mathbf{q}$  plane<sup>6-8</sup> with a rotation angle  $45^\circ$  between the upper and lower branch.

On the theory side there appears to be a consensus that the RP can be interpreted as a low-energy collective antiferromagnetic (AFM) soft mode, becoming undamped (at least underdamped) for  $T < T_c$  due to the onset of the  $d_{x^2-y^2}$  SC gap in the electron-hole excitation spectrum.<sup>10</sup> Two limits of the same scenario seem to be realized. At optimum doping and in slightly underdoped YBCO the resonant mode is weak,<sup>2</sup> indicating that the collective mode is a weakly bound excitonic state within the SC gap.<sup>10-14</sup> On the other hand, at low doping the dominant part of the intensity of spin fluctuations with  $\mathbf{q} = \mathbf{Q}$  is within the RP, so the latter one is closer to an undamped AFM paramagnon mode.<sup>15</sup>

The downward dispersion of the resonant mode is within the random-phase approximation (RPA) and related theories for the dynamical spin susceptibility  $\chi_{\mathbf{q}}(\omega)$  (Refs. 10, 13, 14, and 16) a natural consequence of the closing of the  $d_{x^2-y^2}$  SC gap towards the nodal direction of the Fermi surface (FS). The RPA seems to capture some upward component (silent band) after the disappearance of the downward branch.<sup>14</sup>

In this work we present results of the memory function approach to spin dynamics,<sup>15</sup> which in addition to the above features reproduces the entire upward dispersion observed experimentally at intermediate doping. At the same time, memory function representation offers an appropriate framework (broader than RPA) for the general discussion of the

INS experiments. Thus, it will be shown that the explanation of collective mode properties at low doping implies the existence of a large SC-like pseudogap.

The dynamical spin susceptibility can be generally expressed in the form<sup>15</sup>

$$\chi_{\mathbf{q}}(\omega) = \frac{-\eta_{\mathbf{q}}}{\omega^2 + \omega M_{\mathbf{q}}(\omega) - \omega_{\mathbf{q}}^2}, \quad (1)$$

where the “spin stiffness”  $\eta_{\mathbf{q}} = -i\langle [S_{-\mathbf{q}}^z, \hat{S}_{\mathbf{q}}^z] \rangle$  can be evaluated within models relevant to cuprates,<sup>15</sup> while the “mode frequency”  $\omega_{\mathbf{q}} = (\eta_{\mathbf{q}}/\chi_{\mathbf{q}}^0)^{1/2}$  is related to the static susceptibility  $\chi_{\mathbf{q}}^0 = \chi_{\mathbf{q}}(\omega=0)$ . The latter is a rather sensitive quantity, so we fix it with the fluctuation-dissipation relation<sup>15,17</sup>

$$\frac{1}{\pi} \int_0^\infty d\omega \text{cth} \frac{\omega}{2T} \chi_{\mathbf{q}}''(\omega) = \langle S_{-\mathbf{q}}^z S_{\mathbf{q}}^z \rangle = C_{\mathbf{q}}, \quad (2)$$

whereby the correlation function  $C_{\mathbf{q}}$  is better known within relevant models, although not directly measured via INS so far. In the following we base our analysis on the extended  $t$ - $J$  model, i.e., the  $t$ - $t'$ - $J$  model, within which  $C_{\mathbf{q}}$  is as well restricted by the sum rule

$$\frac{1}{N} \sum_{\mathbf{q}} C_{\mathbf{q}} = \frac{1}{4}(1 - c_h), \quad (3)$$

and  $c_h$  is the hole concentration.

Depending on the damping function  $\Gamma_{\mathbf{q}}(\omega) = M_{\mathbf{q}}''(\omega)$ , Eq. (1) is able to deal with the overdamped response in the normal state (NS), with the spin-wave dispersion at higher energies (at low doping), as well as with the RP peak in the SC phase.

Using the method of equations of motion within the  $t$ - $J$  model it has been shown that the collective spin fluctuations decay into electron-hole excitations.<sup>15</sup> This leads to the lowest-order mode-coupling approximation for the damping in the NS

$$\Gamma_{\mathbf{q}}(\omega) = \frac{\pi}{2\eta_{\mathbf{q}}\omega N} \int d\omega' [f(\omega') - f(\omega + \omega')] \times \sum_{\mathbf{k}} w_{\mathbf{kq}}^2 A_{\mathbf{k}}(\omega') A_{\mathbf{k+q}}(\omega + \omega'), \quad (4)$$

where  $w_{\mathbf{kq}}$  is the effective mode-coupling vertex<sup>15</sup> and  $A_{\mathbf{k}}(\omega)$

is the single-particle spectral function. Provided the existence of “hot spots”  $\mathbf{k}_0$  where the FS crosses the AFM zone boundary we assume that at low- $\omega$  quasiparticles (QP) with dispersion  $\epsilon_{\mathbf{k}}$  and weight  $Z_{\mathbf{k}}$  can determine the spectral function  $A_{\mathbf{k}}(\omega) = Z_{\mathbf{k}} \delta(\omega - \epsilon_{\mathbf{k}})$ . This results in a rather constant  $\Gamma_{\mathbf{q}}(\omega)$  within the NS at low- $\omega$  and at  $\mathbf{q} \sim \mathbf{Q}$ . Although it is derived within the specific prototype model, the form of Eq. (4) is quite generic for the damping of the collective magnetic mode in a metallic system, since the lowest-energy decay processes naturally involve the electron-hole excitations close to the FS. It should be noted that similar expressions appear also in theories based on the RPA approach.<sup>11,14</sup> For the SC phase at  $T < T_c$  Eq. (4) has to be generalized to include the anomalous spectral functions<sup>11</sup> leading to

$$\Gamma_{\mathbf{q}}(\omega) \sim \frac{\pi}{2\omega N} \sum_{\mathbf{k}} \bar{w}_{\mathbf{kq}}^2 (u_{\mathbf{k}} v_{\mathbf{k}+\mathbf{q}} - v_{\mathbf{k}} u_{\mathbf{k}+\mathbf{q}})^2 \times [f(E_{\mathbf{k}}) - f(E_{\mathbf{k}} - \omega)] \delta(\omega - E_{\mathbf{k}} - E_{\mathbf{k}+\mathbf{q}}), \quad (5)$$

where  $\bar{w}_{\mathbf{kq}}^2 = w_{\mathbf{kq}}^2 Z_{\mathbf{k}} Z_{\mathbf{k}+\mathbf{q}} / \eta_{\mathbf{q}}$ ,  $u_{\mathbf{k}}$ , and  $v_{\mathbf{k}}$  are the usual Bardeen-Cooper-Schrieffer (BCS) coherence amplitudes,  $E_{\mathbf{k}} = \sqrt{\epsilon_{\mathbf{k}}^2 + \Delta_{\mathbf{k}}^2}$ , and  $\epsilon_{\mathbf{k}} = -2\tilde{t}(\cos k_x + \cos k_y) - 4\tilde{t}' \cos k_x \cos k_y - \mu$  is a renormalized QP band.

In the region of interest, i.e., for  $\mathbf{q} \sim \mathbf{Q}$  we use for simplicity constant  $\bar{w}_{\mathbf{kq}} \sim \bar{w}$  which still depends on the QP band parameters and chemical potential  $\mu$ . In the following we assume values  $\tilde{t}/t = 0.33$ ,  $\tilde{t}'/t = -0.1$ , and  $t \sim 400$  meV, which roughly apply to moderately doped cuprates, and  $\mu$  is related to doping  $c_h$  in the usual way. For the SC gap we assume the  $d_{x^2-y^2}$  form,  $\Delta_{\mathbf{q}} = \Delta_0(\cos q_x - \cos q_y)/2$ .  $\eta_{\mathbf{q}}$  in Eq. (1) is well known from model calculations<sup>15</sup> and generally quite restricted in range, so we take  $\eta_{\mathbf{q}} = 0.5t$ .

Thus we end up with the following adjustable parameters at chosen  $c_h$ : the correlation function  $C_{\mathbf{q}}$ , the effective coupling  $\bar{w}$ , and the maximum SC gap  $\Delta_0$ . The latter is taken phenomenologically in order to get correspondence with experimental data. The coupling  $\bar{w}$ , or equivalently (weakly  $\omega$  and  $\mathbf{q}$  dependent)  $\Gamma_{\mathbf{q}}^0$  within the NS has been derived within the  $t$ - $J$  model<sup>15</sup> leading to  $\Gamma_{\mathbf{Q}}^0 \propto t$ , but significantly renormalized (reduced) due to AFM spin correlations at low doping. Since a controlled analytical calculation of  $\Gamma_{\mathbf{q}}^0$  is difficult to perform, we furtheron take values for  $\Gamma_{\mathbf{Q}}^0$  close to those found numerically in Ref. 17 for the  $t$ - $J$  model. Note that for the appearance of the upper resonant branch it is crucial that  $\Gamma_{\mathbf{Q}}$  is not too large, as seems to be inherent within the RPA,<sup>11,14</sup> which otherwise yields in the intermediate-doping regime formally quite similar expressions to our Eqs. (1) and (5). Finally, the ansatz for  $C_{\mathbf{q}}$  will depend on doping, as we discuss below.

*Intermediate-optimum doping:* Within this regime the collective mode is heavily overdamped in the NS. The indication for the latter is low intensity of the INS in the relevant low-energy window. It is then reasonable to assume the Lorentzian form  $C_{\mathbf{q}} = C_{\mathbf{Q}} / (1 + \tilde{q}^2 / \kappa^2)$  where  $\tilde{\mathbf{q}} = \mathbf{q} - \mathbf{Q}$  and the sum rule, Eq. (3), relates  $C_{\mathbf{Q}}$  and  $\kappa$ . To be specific, we fix for the presented case the “optimum” doping at  $c_h = 0.15$  and  $\kappa = 1.25$  implying  $C_{\mathbf{Q}} \sim 1.0$ . The SC gap is roughly known from experiments and we take  $\Delta_0 = 40$  meV. For results at

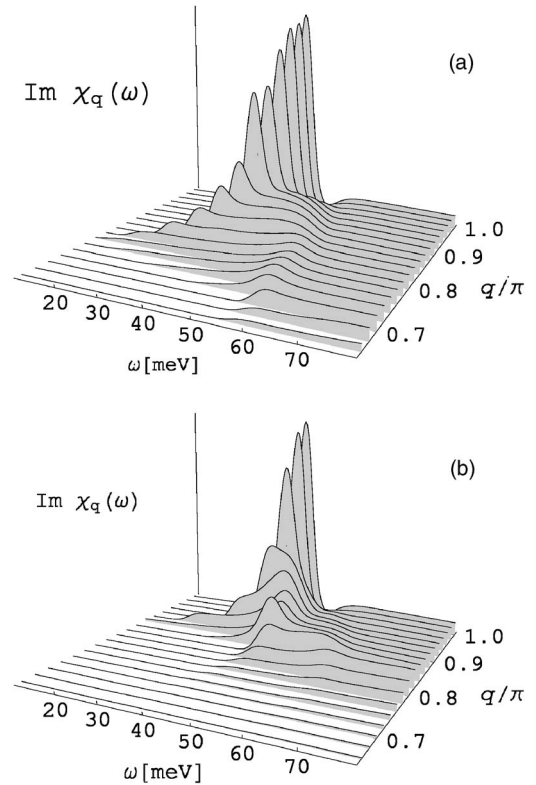


FIG. 1. Magnetic fluctuations spectra  $\chi_{\mathbf{q}}''(\omega)$  (arbitrary units) at intermediate doping  $c_h = 0.15$  for momenta: (a) along the  $x$  direction  $\mathbf{q} = q(1, 0)$  and (b) along the zone diagonal  $\mathbf{q} = q(1, 1)$ .

intermediate doping we use below  $\Gamma_{\mathbf{Q}}^0 \sim 0.45t$  ( $\sim 0.2$  eV).

The spectra in the vicinity of the resonance  $\chi_{\mathbf{q}}''(\omega \sim \omega_r)$  for  $\mathbf{q} \sim \mathbf{Q}$  have been partly studied in Ref. 15. Presented results show besides a pronounced downward dispersion also a weaker upward branch. In Fig. 1 we display  $\chi_{\mathbf{q}}''(\omega)$  for momenta both along the  $x$  axis,  $\mathbf{q} = q(1, 0)$ , and along the zone diagonal  $\mathbf{q} = q(1, 1)$ , while in Fig. 2 we present the planar  $\mathbf{q}$  scans of the intensity  $\chi_{\mathbf{q}}''(\omega)$  at fixed  $\omega$ .

The following observations can be made on the basis of Figs. 1 and 2: (a) both presentations clearly reveal two branches emerging from the same coherent resonant mode at  $\omega_r \sim 41$  meV. Intensity plots of both branches within the  $\mathbf{q}$  plane are squarelike around AFM  $\mathbf{Q}$  (see Fig. 2), however, with quite pronounced anisotropy. (b) For the downward branch the intensities are strongest along the  $(1, 0)$  direction. This is consistent with the faster dispersion along the zone diagonal  $(1, 1)$  [see Fig. 1(a)] which reduces intensity relative to the  $(1, 0)$  direction and deforms the constant  $\omega$  scan into a squarelike pattern. (c) The anisotropy is less pronounced for  $\omega > \omega_r$ , but the overall pattern is rotated through  $45^\circ$ : the dispersion is strongest along the  $(1, 0)$  direction, while intensity is largest along the  $(1, 1)$  direction. (d) Above the damping threshold  $\omega = \Omega_{\mathbf{Q}} \leq 2\Delta_0$  the upward branch merges into an incoherent response broad both in  $\mathbf{q}$  as well as in  $\omega$ . Note, however, that the incoherent part still exhausts most of the intensity sum rule, Eq. (2), even for  $\mathbf{q} = \mathbf{Q}$ .

Let us give some explanation for the behavior of the collective mode as observed in Figs. 1 and 2. At intermediate (near optimum) doping the normal-state damping is large,

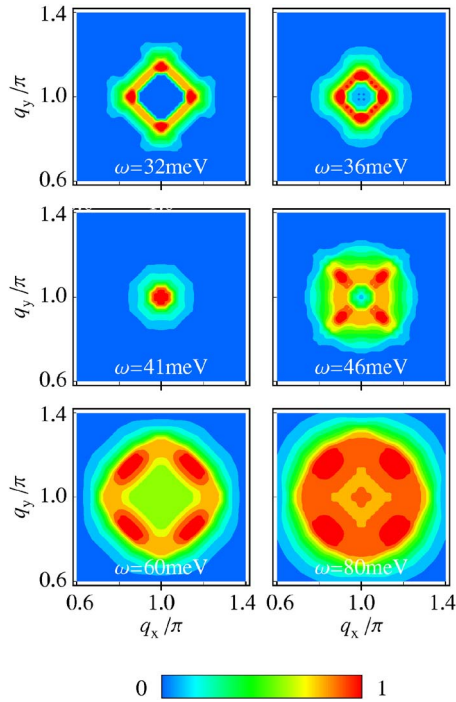


FIG. 2. (Color online) Normalized intensity plot of  $\chi''_{\mathbf{q}}(\omega)$  in the  $\mathbf{q}$  plane at intermediate doping for selected energies  $\omega$  below and above the RP at  $\omega_r \sim 41$  meV.

$\Gamma_{\mathbf{Q}} > \omega_{\mathbf{Q}}$ , and the collective mode is heavily overdamped in the NS. The sharp RP at  $\mathbf{Q}$  appears due to the steplike vanishing damping  $\Gamma_{\mathbf{Q}}(\omega < \Omega_{\mathbf{Q}}) = 0$  within the SC phase, where  $\Omega_{\mathbf{Q}} = 2\Delta_{\mathbf{k}^*}$  and  $\mathbf{k}^*$  represents the location of the hot spot on the FS. Since the damping cutoff is below the characteristic mode frequency,  $\Omega_{\mathbf{Q}} < \omega_{\mathbf{Q}}$ , the character of the resonant mode is excitoniclike,<sup>10,11</sup> i.e., the resonant mode appears below but close to  $\Omega_{\mathbf{Q}}$  and consequently carries only a small part of the whole sum rule, Eq. (2).<sup>15</sup> The dispersion of the mode, both the downward<sup>14,16</sup> as well as the upward one, is intimately related to the properties of the SC gap  $\Delta_{\mathbf{k}}$ . As noted before,<sup>11,14,15</sup> the damping function  $\Gamma_{\mathbf{q}}(\omega)$  shows for  $\mathbf{q} \neq \mathbf{Q}$  several steps, in contrast to a single step at  $\mathbf{Q}$ . Thresholds are determined by the hot spot condition, i.e., by processes of zero-energy electron-hole excitations (in the NS) connecting Fermi surfaces  $\mathbf{k}_{F1} + \mathbf{k}_{F2} = \mathbf{q} + \mathbf{K}$  where  $\mathbf{k}_{Fi}$  are wave vectors on the FS and  $\mathbf{K}$  are reciprocal lattice vectors. Within the SC phase this leads to steps in the damping at  $\Omega_i(\mathbf{q}) = |\Delta_{\mathbf{k}_{F1}}| + |\Delta_{\mathbf{k}_{F2}}|$ . Away from  $\mathbf{q} = \mathbf{Q}$  there are in general four nontrivial  $\Omega_i(\mathbf{q})$ ,  $i = 1-4$ , with a possible degeneracy for  $\mathbf{q}$  with a higher symmetry in the Brillouin zone.

The lowest step at  $\Omega_1(\mathbf{q})$  pushes the downward resonant branch as  $\omega_r(\mathbf{q}) < \Omega_1(\mathbf{q})$ . The latter should for  $\mathbf{q} = q(1, 1)$  approach zero at  $\mathbf{q}_n = 2\mathbf{k}_{Fn}$  where  $\mathbf{k}_{Fn}$  is the nodal point on the FS. It is, however, clear from Fig. 1(b) that the branch loses intensity before reaching this  $\mathbf{q}_n$ . The dispersion of  $\Omega_1(\mathbf{q})$  along the (1, 0) direction is substantially weaker, as seen in Fig. 1(a), which leads to squarelike contours and the (1, 0) dominated anisotropy in Fig. 2. The upper branch in our analysis appears as an exciton-like resonance below next thresholds, i.e.,  $\omega_u(\mathbf{q}) < \Omega_i(\mathbf{q})$ ,  $i > 1$ , where the condition for observing such a resonance is (a) that the finite damping

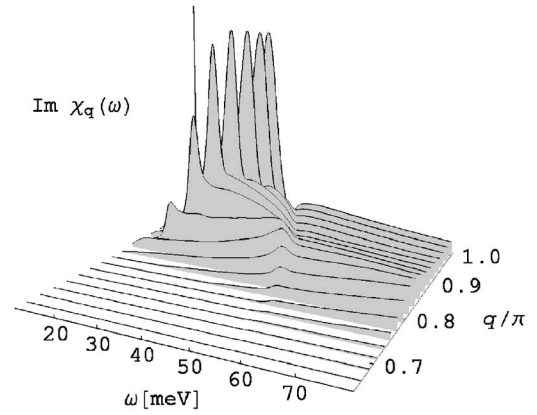


FIG. 3.  $\chi''_{\mathbf{q}}(\omega)$  (arbitrary units) at low doping  $c_h = 0.1$  for  $\mathbf{q} = q(1, 0)$ .

$\Gamma_{\mathbf{q}}(\omega_u)$  is not too large, and (b) that  $\omega_u^2/\Gamma_{\mathbf{q}}^0 \geq \Omega_4(\mathbf{q})$ . The latter condition is necessary to insure that a measurable amount of spectral weight builds up at threshold  $\Omega_i(\mathbf{q})$  by way of Eq. (2). Finally, for  $\omega > \Omega_4(\mathbf{q})$  the damping  $\Gamma_{\mathbf{q}}(\omega)$  is large and quite constant and any resonant features disappear into the strongly overdamped AFM paramagnonlike background.

*Low-doping:* As already noted, at low doping the effective vertex  $\bar{w}$  is reduced due to enhanced AFM fluctuations resulting in a smaller normal-state damping  $\Gamma_{\mathbf{Q}}(\omega)$  (Refs. 15 and 17) but also in larger  $C_{\mathbf{Q}}$ , which induces spin-wavelike dispersion at larger  $\omega$ , as observed in INS experiments.<sup>8,9</sup> Both facts lead to lowering of  $\omega_{\mathbf{Q}} \propto c_h$ ,<sup>15</sup> which at the same time corresponds closer to the resonance  $\omega_r \sim \omega_{\mathbf{Q}}$ . Moreover, the resonance peak exhausts substantial part of the sum rule. To account for the spin-wavelike dispersion at  $\tilde{q} > \kappa$  and a possible influence of a weak incommensurability  $\delta_i = (\pm\delta, 0), (0, \pm\delta)$  we assume

$$C_{\mathbf{q}} = A \sum_i^4 \frac{1}{\sqrt{\kappa^2 + 3|\mathbf{q} - \mathbf{Q}_i|^2}}, \quad (6)$$

where  $\mathbf{Q}_i = \mathbf{Q} + \delta_i$ , and  $A$  is fixed by the sum rule, Eq. (3). In contrast to intermediate doping, a direct application of the damping, Eq. (4), with a single SC gap seems not to be sufficient to describe the observed INS results. First, the RP in underdoped YBCO appears to remain broad (not resolution limited) for  $T < T_c$ , compatible with a finite damping persisting in the SC phase.<sup>2,3,9</sup> Still, there is some signature of a double dispersion,<sup>9</sup> although the downward dispersing mode is much less pronounced.

To account for these observations, we generalize at low doping the damping function  $\Gamma_{\mathbf{q}}(\omega)$ , Eq. (5), as follows. Inside the SC (pseudo) gap, i.e., for  $\omega < \Omega_1(\mathbf{q})$ , we assume a finite damping  $\Gamma_{\mathbf{q}}^c(\omega)$ . Although at low doping there are some indications for the existence of yet another (spin) gap  $\omega_c < \omega_r$ ,<sup>2,3,9</sup> whereby  $\Gamma_{\mathbf{q}}^c(\omega < \omega_c) = 0$ , a potential dispersion of  $\Gamma_{\mathbf{q}}^c(\omega > \omega_c)$  does not have any significant effect on the RP and we assume further for simplicity a constant  $\Gamma^c$  throughout the pseudogap.

In Figs. 3 and 4 we display results for low  $T \sim 0$ , corresponding to low doping  $c_h \sim 0.1$ , where following parameters



have been adopted:  $\kappa = \delta = 0.3$  (implying  $C_Q \sim 1.6$ ), damping  $\Gamma_Q^0 = 60$  meV,  $\Gamma^c = 18$  meV, and the SC (pseudo) gap  $\Delta_0 = 38.5$  meV. While  $\kappa$  and  $\Delta_0$ , and even  $\Gamma^c$ , are accessible from experimental data,  $\Gamma_Q^0$  has been chosen to still reproduce the spin-wavelike response observed experimentally at higher energies. This causes the upward dispersion to become stronger as compared to intermediate doping (Figs. 1 and 2) while RP becomes broader due to finite  $\Gamma^c$ , but still underdamped. There is also a signature of a downward branch with the same anisotropy as for the intermediate doping, but less pronounced and losing fast in intensity.

Let us further discuss the correspondence of presented results with INS data on cuprates. Within the presented memory function approach two distinctive regimes emerge depending mainly on the NS damping  $\Gamma_Q^0$  and on the correlation length  $\kappa$ . Both are doping sensitive,<sup>17,18</sup> whereas the SC (pseudo) gap  $\Delta_0$  remains approximately constant throughout the low to intermediate doping regime. Thus for intermediate doping where the NS response is strongly overdamped, reflecting both large  $\Gamma_Q^0$  and  $\kappa$ , our results agree with features seen in optimum or slightly underdoped YBCO well below  $T_c$ :<sup>5-7</sup> (a) a sharp RP of small integrated intensity appearing slightly below the lower edge of an otherwise featureless continuum, (b) pronounced downward dispersion with an enhanced intensity along the (0, 1) direction, and (c) broader and less pronounced upward dispersive branch with somewhat stronger intensity along the (1, 1) direction in a narrow energy range above  $\omega_r$ . While all the above features also appear in INS experiments on underdoped cuprates, e.g. in underdoped YBCO,<sup>8,9</sup> there are also some important differences: (a) the downward dispersion is less pronounced, while the upward dispersion evolves into spin waves at higher  $\omega$ , and (b) the RP appears well below the threshold energy  $\Omega_Q$  and acquires a finite width. Within the present approach with  $\Gamma_Q^0$  and  $\kappa$  as the only relevant parameters such a scenario is possible only if  $\Gamma_Q^0$  is substantially reduced due to AFM spin fluctuations from its value at optimal doping. Moreover, a finite RP peak width and large integrated intensity seem to imply a nonvanishing damping  $\Gamma^c$  inside the SC pseudogap. Here the sum rule of Eq. (2) becomes particularly effective and tends to suppress the downward dispersion unless  $C_q$  itself becomes incommensurate.

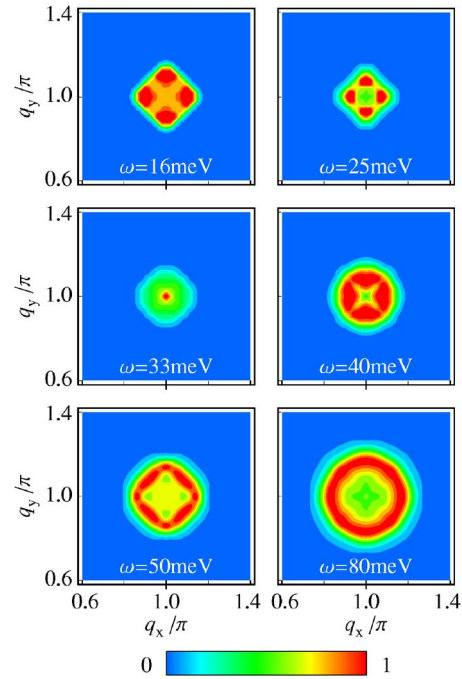


FIG. 4. (Color online) Normalized intensity plot of  $\chi''_q(\omega)$  in the  $q$  plane at low doping. The RP is at  $\omega_r \sim 33$  meV.

In conclusion, we have shown that the RP double dispersion and its anisotropy are a nontrivial consequence of the damping  $\Gamma_q(\omega)$  in the SC phase, reflecting the nature of the gap  $\Delta_q$  and related thresholds  $\Omega_q(\mathbf{q})$ . In this sense, the INS results on RP serve as a very stringent test for the mechanism of the collective mode decay and the structure of the SC gap. While our basic assumption<sup>15</sup> of the decay into electron-hole excitations, consistent with other authors,<sup>11,14</sup> does not offer much freedom of interpretation at intermediate doping,<sup>10-14</sup> at low doping an AFM spin-fluctuation scenario seems more appropriate. We get a reasonable explanation of experiments only after assuming a finite damping  $\Gamma^c$  within the SC pseudogap. We should point out that a similar quasi-universal development is observed even in non-SC cuprates.<sup>19</sup>

<sup>1</sup>J. Rossat-Mignod *et al.*, Physica C **185-189**, 86 (1991).

<sup>2</sup>P. Bourges, in *The Gap Symmetry and Fluctuations in High Temperature Superconductors*, edited by J. Bok, G. Deutscher, D. Pavuna, and S. A. Wolf (Plenum, New York, 1998).

<sup>3</sup>H. F. Fong *et al.*, Phys. Rev. B **61**, 14 773 (2000); P. Dai *et al.*, *ibid.* **63**, 054525 (2001).

<sup>4</sup>P. Bourges *et al.*, Science **288**, 1234 (2000).

<sup>5</sup>M. Arai *et al.*, Phys. Rev. Lett. **83**, 608 (1999).

<sup>6</sup>S. Pailhès *et al.*, Phys. Rev. Lett. **93**, 167001 (2004).

<sup>7</sup>D. Reznik *et al.*, Phys. Rev. Lett. **93**, 207003 (2004).

<sup>8</sup>S. M. Hayden *et al.*, Nature (London) **429**, 531 (2004).

<sup>9</sup>C. Stock *et al.*, Phys. Rev. B **69**, 014502 (2004); C. Stock *et al.*, *ibid.* **71**, 024522 (2005).

<sup>10</sup>M. Lavagna and G. Stemmam, Phys. Rev. B **49**, 4235 (1994).

<sup>11</sup>D. K. Morr and D. Pines, Phys. Rev. Lett. **81**, 1086 (1998).

<sup>12</sup>J. Brinckmann and P. A. Lee, Phys. Rev. Lett. **82**, 2915 (1999).

<sup>13</sup>M. R. Norman, Phys. Rev. B **61**, 14 751 (2000).

<sup>14</sup>I. Eremin *et al.*, Phys. Rev. Lett. **94**, 147001 (2005).

<sup>15</sup>I. Sega, P. Prelovšek, and J. Bonča, Phys. Rev. B **68**, 054524 (2003).

<sup>16</sup>A. V. Chubukov, B. Janko, and O. Tchernyshyov, Phys. Rev. B **63**, 180507(R) (2001).

<sup>17</sup>P. Prelovšek, I. Sega, and J. Bonča, Phys. Rev. Lett. **92**, 027002 (2004).

<sup>18</sup>J. Bonča, P. Prelovšek, and I. Sega, Phys. Rev. B **70**, 224505 (2004).

<sup>19</sup>J. M. Tranquada *et al.*, Nature (London) **429**, 534 (2004).